EVALUATING THE E-PERM RT CHAMBER FOR USE MEASURING RN-220 IN A CAVE ENVIRONMENT

Lawrence E. Welch*, Emma J. Art, Garrett D. Rau, Matthew J. Frana, Edward C. Klausner, Elizabeth R. Miller, Mark D. Jones, and Michael J. Lace
Knox College
Galesburg, Illinois, USA
lwelch@knox.edu

Abstract

Standard E-PERM sensors respond mainly to Rn-222, with only a small percentage of any Rn-220 being detected due to most of these isotopic species decaying prior to diffusing into the chamber interior. The RT chamber was designed to allow most of the Rn-220 to be counted, while still responding fully to Rn-222. Construction of the RT chamber involves cutting circular holes in the thermoplastic side walls of a standard S chamber and covering them with a layer of Tyvek, which provides a new and more rapid diffusion route for airborne radon to enter the chamber after it has been opened. This study probes whether the structural modification of the S chamber to shorten radon diffusion time also alters the degree of background radiation shielding provided, and whether this impacts cave radon measurements.

(1) The authors have received partial funding from Knox College to support the research leading to this publication, including allocations from the Billy Geer Fund, the Andrew W. Mellon Foundation, the Committee on Faculty Research, and the Paul K. and Evalyn Elizabeth Cook Richter Trusts.

Introduction

Electret Ion Chamber (EIC) radon sensors provide a reliable way to measure integrated average radon levels without needing a power source and in a much less expensive package than with use of a continuous radon monitor (CRM) (Kotrappa, 1988, 1990). The EIC sensors have proven to be robust when faced with challenging sampling environments over a wide temperature range, particularly for damp, high-humidity sites (Welch, 2016). EIC sensors are commercially available as E-PERM brand units from Rad Elec. One can assemble a completed E-PERM with one of a handful of chamber styles, featuring a range of volumes, thus producing different sensitivities. There are also three different electret types, each with a different bulk of surface charge, which also allows customization of the sensitivity to radon. All the E-PERM sensors have no pump, so radon enters the chamber passively via whatever gaseous advection is present in the sampling environment. The standard S chamber only detects 3% of the ^{220}Rn isotope while responding quantitatively to ^{222}Rn due to the requirement of passive gas entry (Stacks, 2015). The half-lives are 55.6 seconds and 3.823 days for ^{220}Rn and ^{222}Rn respectively (Rumble, 2018). Most of the ^{220}Rn that enters the chamber decays while passing through the inlet filter, and thus is not detected by the sensor. Knowing that the half-life of ^{220}Rn is 55.6 sec, and assuming that only 3% of it passes through the filter, one can solve mathematically that 97% of the ^{220}Rn decays in 281 sec. Thus, 281 seconds would serve as a good estimate of the delay time for radon to pass through the inlet filter of the chamber to reach the active element of the sensor. This is sometimes referred to as the latency of the sensor. All other radon isotopes have more diminutive half-lives than ^{220}Rn, thus are too short to register any signal with an E-PERM featuring an S chamber.

For those interested in quantitatively measuring ^{220}Rn in addition to ^{222}Rn, Rad Elec offers the RT chamber as an option for its E-PERM system. The RT chamber is a modified S chamber, featuring a row of circular pores, 18 mm in diameter, cut into the thermoplastic lower flange of the S chamber, which are then covered with a layer of 0.13 mm thick Type 14 Tyvek (Stacks, 2015 and Kotrappa, 2010). Radon is known to diffuse rapidly through this Tyvek layer (each layer is estimated to delay gas passage into the chamber by about 8 seconds (Kotrappa, 2014)), permitting an E-PERM equipped with an RT chamber to respond quickly enough to quantitatively measure environmental ^{220}Rn. The RT chamber should provide an integrated average of ^{220}Rn and ^{222}Rn combined, so running an RT chamber side-by-side with an S chamber offers the possibility of calculating the concentrations of both Rn isotopes by measuring the difference in responses.

Past work in this research group has pursued measurement of radon in caves and correlation of the differing radon levels with various environmental variables (Welch, 2015-2019). A recent study compared airborne cave radon concentrations with uranium and thorium concentrations in the adjacent cave rock, soil, and water (Welch, 2021). One notable result of this study was that high radon concentrations were found in caves featuring relatively low levels of uranium and thorium. The cave soils had much more thorium present than uranium, and it provoked thoughts

about whether a significant amount of ^{220}Rn (a decay product of thorium whereas ^{222}Rn comes from uranium) was being missed, given prior use of E-PERM sensors with standard S chambers, which only detect 3% of this isotope, along with CRM usage that would see none of it due to lengthy sensor latency. As such, acquisition of some RT chambers for use undertaking side-by-side trials run versus S chambers was an attractive option to evaluate ^{220}Rn content. Early in-cave trials with this approach confirmed that the RT chambers consistently produced higher calculated radon concentrations than proximate S chambers. Prior to accepting that this excess was solely due to the ^{220}Rn that was not being measured before, it seemed prudent to evaluate other potential sources of this excess signal. In particular, the modification of the S chamber to construct an RT chamber, where disks of thermoplastic were replaced with Tyvek-covered pores, looked to potentially alter the shielding of ionizing radiation from outside the chamber. The current study was designed to evaluate whether the RT chamber had a significantly different degree of shielding to external ionizing radiation than a standard S chamber, and if there was a difference whether it was likely to be a significant factor in the cave environments being evaluated by this research group.

Materials and Methods

Integrated average radon concentrations were measured with E-PERM® EIC (Electret Ion Chamber) sensors, consisting of an electret of either the short-term [ST] or long-term [LT] variety, and a chamber of either the S or RT variety, all from Rad Elec Inc. A modified-RT chamber was constructed by screw-mounting a cylindrical ring of 6 mm thick and 40 mm high schedule 40 PVC around the base of the RT chamber producing an average gap of 9 mm between the inside of the PVC belt and the external wall of the RT chamber itself. The gap still allowed free gaseous circulation to the underlying chamber walls. Figure (1) shows the three different chamber types; the Tyvek-covered pores added to the RT chamber can be seen lining the lower flange outlined against the gray Tyvek. All chamber volumes were 210 ml. Electret voltages were measured with a SPER-1E electret voltage reader (Rad Elec). Calculations were done with Radon Report Manager Software Version 3.8.44 from Rad Elec. Background gamma radiation exposure was evaluated with the Model 2 Gamma Ray Dosimeter manipulated with the Model 909B charger from Arrow-Tech.

Temporal measurements of radon concentration were undertaken using Radon Recon CRM (Continuous Radon Monitor) sensors and Recon Download Tool software v0.9.7 (Rad Elec Inc.). Recon measurements were acquired at 10-minute increments rather than the standard 1-hour increment via spreadsheet manipulation of the raw data file.

Figure (1): E-PERM chambers used, left to right: S, RT, modified-RT.

Sealed low-level radioactive pellets with activities below regulatory limits were obtained from Spectrum Techniques. The alpha source was a new pellet containing 0.1 μCi of ^{210}Po, which has an alpha decay energy of 5.407 MeV. The beta source was an older pellet of ^{90}Sr with a beta decay energy of 0.546 MeV, producing a ^{90}Y decay product with a beta decay energy of 2.28 MeV. The pellet was rated at 0.1 μCi when it was new in January 2008, so during the time span of actual use the pellet had an activity of circa 0.07 μCi. The gamma source was a new pellet containing 1 μCi of ^{57}Co, with a primary gamma energy of 0.12206 MeV along with a handful of less prevalent gamma emissions (Rumble, 2018). During shielding experiments, the pellets were placed at measured distances in one of four different positions relative to the chamber: above, below, parallel, and diagonal above. Figure (2) illustrates each of these positions. The above position should be comparable for all three chamber types, as would be the below position. It should be noted that, whereas the shielding from the above position would be from the chamber wall itself, the below position would feature shielding from the electret, which is screwed into the bottom of the chamber. The parallel position has the pellet directly in line with the Tyvek-covered pores bored into the original S chamber to create the RT chamber. In the modified-RT chamber, the radiation from the pellet in the parallel position would have to pass through the added band of PVC prior to reaching the chamber walls. The S chamber shielding in the parallel position would be expected to be the same as that in the above position. The diagonal above position points the pellet at the Tyvek-covered pores of the RT chamber but from a sharp angle above. This angle would enable some of the radiation to bypass the PVC belt of the modified-RT chamber. The standard pellet experiment involved placing the pellet at a measured distance from one E-PERM in one of the given geometries (see Fig (2)), and then compared to the average of three control E-PERMs of the same type in the same environment at the same time without the pellet. Shielding studies were done in a laboratory that had only a tiny amount of ^{222}Rn and where ^{220}Rn had never proven to be measurable and was presumed to be effectively at zero concentration.

A

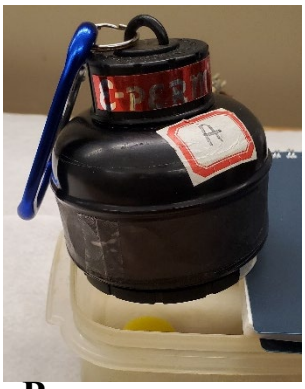

B

C

D

D

Figure (2): Different radioactive pellet orientations around the E-PERM. A) Above. B) Below. C) Parallel. D) Diagonal above.

The Geiger counter was a Series 900 Mini-monitor from Mini-Instruments LTD. Unless a distance is stated with the provided data, the detector head of the Geiger counter was placed directly on the sample. To evaluate the contribution of alpha radiation within the Geiger signal, all measurements were repeated with a piece of standard printer paper, known to block most alpha radiation passage, placed between the detector head and the sample.

The E-RPISU unit was from Rad Elec. For this work, it was not used as intended to measure the equilibrium factor of radon with its progeny, but rather it provided a pump-and-filter unit for

sampling airborne particulates. Gaseous flow rates of 0.8 liters per minute were utilized for all filter trials, and the filter chosen was made from a borosilicate glass matrix with 1 micrometer pore size. Evaluation of the background signal from particulates in Coldwater and Kemling Caves was done by using a pump to pull cave air through a piece of filter paper for a fixed duration at the standard flow rate, then the filter paper was removed and taped directly against one of the Tyvek-covered pores of an RT chamber with the accumulation side of the filter pointed inward, and an E-PERM trial run undertaken. The experimental sampling site for the E-PERM was outside the cave, essentially a blank environment, so any signal resulting from the trial would presumably be from the particulates deposited on the filter. This signal was then compared to a control signal from an E-PERM with an RT chamber featuring an unused piece of filter paper taped to it in the same manner as the experimental sensor and run at the same site.

To minimize the impact of human visitation on the cave atmosphere in Coldwater Cave, the entrance was sealed immediately after human entry and exit, and kept closed throughout the experimental trials. Since Kemling Cave was naturally open to the outside atmosphere, there was no need for special airflow protocol during its visitation. The layouts of both caves and the descriptions of the sampling sites used in them have been described in detail in a previous paper (Welch, 2021).

Results and Discussion

Pellet Shielding Studies

The default assumptions about shielding provided by the E-PERM chamber were that the chamber would filter out all the easily blocked external alpha radiation and most of the more-penetrating beta radiation; whereas, external gamma radiation faced only minimal blockage by the chamber walls and thus needed a correction term in the algorithm for calculating radon concentration from raw E-PERM voltage data. The only real concern with external alpha radiation was whether the thin layer of Tyvek covering the pores in the lower flange of the RT chamber was a sufficient barrier, as there was no question about the thermoplastic shell prohibiting entry. For reference, the ^{210}Po alpha pellet registered 180 counts per second (cps) when placed 1 cm away from the Geiger counter head, yet the signal dropped to the laboratory background of less than 1 cps when a single sheet of printer paper was inserted between pellet and detector head. Table 1 summarizes the alpha pellet shielding results, with the ΔSignal term representing calculated radon concentration in pCi/L for the pellet-irradiated sensor minus the calculated average radon concentration of the control group. When the alpha pellet was placed 5 cm away in the parallel position, making it point directly at the Tyvek-covered pores for the RT chamber, it did not lead to a significant signal increase compared to the control group for the either the RT or the S chamber. When the pellet was moved in to just 1 cm from the chambers, the same result was obtained. So, the Tyvek layer did provide sufficient shielding from external alpha radiation, and it can be concluded that external alpha is not a factor for either S or RT chambers.

Table 1: Alpha pellet data for S and RT chambers.

Chamber Type	Pellet Position	Pellet Distance (cm)	Average ΔSignal (pCi/L)
S	parallel	5	<0
RT	parallel	5	0.5
S	parallel	1	0.1
RT	parallel	1	0.3

Since full shielding from external beta radiation appeared less of a certainty, beta pellet studies were undertaken in all four of the geometries shown in Figure (2). For reference, the ^{90}Sr beta pellet registered 450 cps on the Geiger counter from a distance of 1 cm, and 100 cps from 5 cm; paper shielding had minimal impact on these values. Table 2 summarizes the outcomes of these trials. The most obvious conclusion that can be drawn from these data is that the standard S chamber does not completely shield against signal from external beta radiation. The only exception is for the below position, but in this case the shielding is from the electret itself rather than the chamber walls. The embedded aluminum in the electret is likely the reason for the improved shielding compared to the thermoplastic of the chamber (Stacks, 2015). The other three positions produced a modest, yet significant, increase in signal from the 5-cm distance for the S chamber. The 5-cm RT chamber data looked similar to the S chamber outcomes for the above and below positions, which makes sense given that the parts of the chamber that provide shielding for these geometries would be the same for both S and RT types. When the pellet was

Table 2: Beta pellet data for S, RT, and modified-RT chambers.

Chamber Type	Pellet Position	Pellet Distance (cm)	Average ΔSignal (pCi/L)
S	below	5	< 0
RT	below	5	< 0
S	above	5	4.6
RT	above	5	5.4
S	diagonal above	5	8.4
RT	diagonal above	5	11.9
S	parallel	5	5.8
RT	parallel	5	20.5
S	parallel	15	2.0
RT	parallel	15	6.7
S	parallel	25	1.2

RT	parallel	25	1.8
S	parallel	35	< 0
RT	parallel	35	< 0
Modified-RT	parallel	5	1.4
Modified-RT	diagonal above	5	9.0

moved to the parallel or diagonal above positions, the RT chambers had larger ΔSignal values than the S chambers. The parallel position had the pellet directly in line with the Tyvek-covered pores, and the diagonal above position had the pellet pointing at the new openings on the RT chamber but from a sharp angle above. Clearly, the Tyvek provided less beta shielding than the thermoplastic shell of the chamber. It can be noted that the ΔSignal value for the diagonal above of the S chamber was slightly higher than the above position value. The 5-cm spacing was measured along the diagonal path, which meant that the pellet was less than 5 cm from the side wall of the chamber at its closest approach, thus the elevated signal. When the pellet was moved farther away while kept in the parallel position, the expected reduction in ΔSignal was observed. Pellet distances beyond 25 cm did not impact the output for either chamber type. Whereas the ^{90}Sr pellet certainly was much too active to represent a typical background signal, it does suggest that some concern about sampling environment beta radiation background is warranted. It should be noted that the training manual for use of the E-PERM devices suggests that the units should be deployed at least 20 inches above the floor and 12 inches from an external wall – advice which, if followed, should eliminate interference from all background beta environments except those more active than the ^{90}Sr pellet (CERTI, 2006). Environmental analysts could place samples consistent with this advice by using tripods or sampling stands to hold the E-PERM units.

Although there was no question that background gamma radiation would penetrate through the walls of an E-PERM in use, this was less of a concern than potential background signal from other modes of radiation, as measured background gamma exposure was corrected for within the standard radon calculation algorithm for the E-PERM system. Experience with cave environments has shown that the gamma background correction would be a very minor factor unless the cave radon concentration was unusually low. So gamma permittivity was a given, meaning the biggest concern for this study was whether the RT chamber would feature different permittivity as compared to the unmodified S chamber. For reference, the ^{57}Co gamma pellet registered 35 cps on the Geiger counter from a distance of 1 cm, and 6.5 cps from 5 cm; paper shielding had minimal impact on these values. Table 3 summarizes the outcomes from the gamma pellet trials. When the pellet was at 5 cm from the chambers, the RT chambers started to show greater ΔSignal values versus the controls than the S chambers. Since the gamma pellet was much less active than the beta pellet via Geiger counter measurements, a set with the pellet at 1 cm distance in the parallel position was added. This showed a much more dramatic

difference between the two chamber types. As with the beta experiments, gamma sources distant from the chambers did not produce added signals compared to the controls, so the same advice given above regarding placing the E-PERM units away from surfaces would help minimize any concerns from gamma background as well.

Table 3: Gamma pellet data for S and RT chambers.

Chamber Type	Pellet Position	Pellet Distance (cm)	Average ΔSignal (pCi/L)
S	parallel	1	1.8
RT	parallel	1	12.0
S	parallel	5	0.4
RT	parallel	5	1.8
S	parallel	15	0.2
RT	parallel	15	0.4

As described in the Materials and Methods section and depicted in Figure (1), a modified-RT chamber was constructed that had a band of PVC occluding the Tyvek-covered pores of the RT chamber. By design, the added PVC would provide additional shielding for pellet sources in the parallel position, but pellets placed in the diagonal above position would have greater access to the Tyvek-covered pores compared to parallel, and thus only a partial increase in shielding would occur in this geometry. Data at the bottom of Table 2 using a beta pellet confirmed this mode of response for the modified-RT chamber. The additional PVC brought the parallel beta pellet signal down to nearly the level of the control average; whereas, diagonal above with the modified-RT gave a response intermediate between S and RT. So, a portion of the pellet signal was being filtered out by the PVC, yet a portion was able to bypass the PVC and reach the Tyvek-covered pores with their higher permittivity. When placing the modified-RT chamber in a normal sampling environment, it was important to remember that the added PVC only provided additional shielding to radiation coming from a limited access cone of angles from the 3-dimensional space around the chamber. If the external beta signal were significant, use of the modified-RT would be expected to yield less calculated radon than an RT chamber by a significant amount. If the external beta signal were not significant, the modified-RT chamber would be expected to produce a calculated radon signal similar to the RT chamber, which would be greater than the value from the S chamber if ^{220}Rn were present.

Geiger Counter Measurements

A considerable amount of E-PERM data had been collected previously in Coldwater Cave and Kemling Cave in Iowa by placing the E-PERM units directly on the cave floor, rather than tripod-mounting them (Welch, 2021). Was the background beta and gamma radiation high enough in these caves to make the differential in shielding between the S and the RT chambers a factor? The caves were in the same geologic strata and were known to sport high radon concentrations, yet were relatively low in uranium and thorium concentration. A survey of the primary sampling location in each of the caves with a Geiger counter was undertaken to get an overview of the background radiation, with data displayed in Table 4. The difference in general Geiger activity between the two caves was startling, and it was noteworthy that the alpha contribution, which should be the difference between the raw Geiger reading and the reading with the added sheet of paper, was small in all cases. The cave air in Kemling Cave was similar in radiation counts to the solid surfaces within the cave, but the air in Coldwater Cave appeared to produce much less radiation than the solid surfaces within the cave. However, the solid surfaces within Coldwater Cave produced large counts, and certainly spawned concerns regarding the difference in shielding for the S and RT chambers.

Table 4: Geiger counter results from Kemling Cave and Coldwater Cave surfaces.

Kemling Cave Station K-34R			Coldwater Cave Station 4		
Sample	Station Value (cps)	Station through 1 layer paper (cps)	Sample	Station Value (cps)	Station through 1 layer paper (cps)
Surface Air	0.8	0.8	Surface Air	0.8	0.8
Cave Air	2.3	2.3	Cave Air	7.0	6.0
Cave Rock 1	2.5	2.0	Cave Rock 1	32	27
Cave Rock 2	2.0	2.2	Cave Rock 2	26	19
Cave Rock 3	3.0	2.8	Cave Rock 3	18	13
Cave Formation 1	3.5	3.0	Cave Formation 1	23	18
Cave Formation 2	3.0	3.4	Cave Formation 2	15	15
Cave Formation 3	2.7	3.2	Cave Formation 3	42	38
Cave Soil 1	3.3	3.0	Cave Soil 1	22	19
Cave Soil 2	4.0	4.0	Cave Soil 2	19	17
Cave Soil 3	4.3	3.8	Cave Soil 3	21	21

Particulate Studies

Cave gases were presumed to be less likely to provide significant beta and gamma background signals than the solid cave surfaces, and the Coldwater Cave Geiger data affirmed this notion. Certainly, the standard gases making up the air were unlikely sources for high radioactive signals. Both study caves had been discovered to have atmospheres greatly enriched in carbon dioxide as compared to the standard surface air composition (Welch, 2019), which could provide enhanced beta background via the ^{14}C content of this gas. However, studies placing E-PERM units in chambers with pure carbon dioxide showed no elevation in signal compared to control readings, so standard air gas mixtures, even with elevated carbon dioxide, were ruled out as a significant background radiation source. Airborne particulates presented a more likely candidate as a source of beta and gamma radiation. Table 5 summarizes the outcome of the particulate trials in Coldwater and Kemling caves using the methodology from the Materials and Methods section. The Δsignal column represents the cave E-PERM minus the control E-PERM in units of calculated radon concentration. It should be noted that the Coldwater Cave trials were all collected within a 24-hour time frame, and the Kemling Cave trials were collected on different dates spread well apart in time. Prior work has revealed that Coldwater Cave has relatively constant radon levels over short time frames, and Kemling Cave has highly variable temporal radon concentrations (Welch, 2021). Although this experiment did not measure airborne radon, both the radon levels and the particulate radioactivity levels vary as a function of the movement of air masses through the caves. Coldwater has very slow air turnover, so the airborne particulate levels should have been relatively constant in the three trials included in Table 5, producing the obvious progression with accumulation time. Kemling Cave at station K-34R has much more rapid air turnover, and given that the three trials from this cave were done on differing dates, the signal from this experiment as a function of accumulation time does not show a progression. Clearly, the particulates do provide some degree of background signal; although, the signal was very small compared to the radon signals in these caves, as the Kemling Cave station K-34R of 210.0 pCi/L average radon concentration and Coldwater Cave station 4 average of 508.6 pCi/L (Welch, 2021) greatly overshadow the particulate signals and their variability.

Table 5: Cave air particulate background signal after accumulation on filter paper.

Kemling Cave Station K-34R		Coldwater Cave Station 4	
Accumulation Time (hours)	Average ΔSignal (pCi/L)	Accumulation Time (hours)	Average ΔSignal (pCi/L)
3	3.2	3	<0
6	2.8	6	1.6
9	0.8	9	6.3

Modified-RT Trials

Cave trials utilizing the modified-RT chamber side-by-side with S and RT chambers gave an opportunity to probe the impact of the differential shielding of the different chambers. Whereas the additional PVC layer of the modified-RT offered greater shielding from radiation generated by remote surfaces in the cave, airborne particulates would be able to flow behind the PVC shielding, and their betas and gammas could have direct access to the Tyvek-covered pores in the RT sensor flange from a short distance away. Normal cave trials with E-PERMs have been done with multiple sensors run in parallel to improve the precision of the output. Multiple RT and S chambers could be mustered for a cave trial, but there was only one modified-RT chamber available, so no replicates were possible for this measurement during a single trial. As such, the side-by-side experiment comparing the three different chambers was run six times to improve the precision of the conclusions gathered from the trials. Each trial featured the single modified-RT sensor alongside sets of at least four S and four RT sensors. The summary of the outcome of these trials at a location collected in Kemling Cave is shown in Table 6. As a reference, data from concurrent Recon CRM trials have also been included in Table 6. The long latency period for gas introduction into the Recon units (Welch, 2019) meant that they would not detect any ^{220}Rn, so the Recon radon concentration readings would be expected to yield values similar to or slightly below the S chamber values, which only sense 3% of the ^{220}Rn. As expected, the Recon yielded data very similar to the S chambers; whereas, the RT and modified-RT values were similar to each other and circa 6% elevated from the S chamber reading. This suggests that the PVC belt added to the modified-RT chamber was not significantly reducing the radiation background reaching the inside of the RT chamber, which implies that betas and gammas from remote surfaces in the cave were not a significant issue. Radiation from particulates could not be ruled out as contributing to the absolute difference between the RT chambers and the S chamber. Although vapors and particulates could reach the space behind the PVC piece, it seemed likely that if the background radiation signal from particulates were a factor, the modified-RT would at least provide partial shielding from those particulates outside the PVC belt. The similarity in radon concentration values between the RT and the modified-RT chamber suggested that background radiation contribution to the overall signal was likely not a factor.

Table 6: Data for cave trials of the modified-RT chamber vs. RT and S chambers at the same location, Kemling Cave, Station K-34R.

Absolute Values (pCi/L)	
Absolute Recon	293.8
Absolute S Chamber Avg	293.9
Absolute RT Chamber Avg	310.8
Absolute Modified-RT Chamber Avg	311.6
Absolute Comparison (pCi/L)	
Absolute change, S vs Recon	0.1
Absolute change, RT vs S	16.9
Absolute change, RT vs Recon	17.0
Absolute change, Mod-RT vs RT	0.8
Absolute change, Mod-RT vs S	17.7
Relative Comparison (%)	
% change, S vs Recon	0.05%
% change, RT vs S	5.76%
% change, RT vs Recon	5.81%
% change, Mod-RT vs RT	0.25%
% change, Mod-RT vs S	6.02%

Hanging E-PERM Trial

One final type of experiment was run to probe the impact of background radiation in the cave sampling environment. A series of four replicate experiments had already been run at Coldwater Cave station 4 doing side-by-side measurements with a series of four RT chambers versus four S chambers. These E-PERMS were placed with their bottoms directly on a rock shelf, and with some side exposure to rock surfaces within less than a meter. If the cave surfaces were beta and gamma emitters, then there was the potential of exposure through the Tyvek-covered pores. For comparison with these trials, a separate trial was run with a rope suspended across the tall canyon passage about 10 meters downstream of station 4, and E-PERM units with four replicate RT and S chamber E-PERMs suspended from the rope via nylon webbing (see Figure (3)). The sensors could be mounted and turned on and off from the floor by creating slack in the transverse line, then the rope was pulled taut to suspend the sensors away from cave surfaces while the experiment was run. The final positioning of the sensors placed them hanging in space, isolated from the nearest cave surface by 1.8 meters at a minimum. Given the penetrating distance of beta radiation in air of 3.7 meters per MeV of energy (Ionactive, 2021), this distance ensured that

only the most energetic betas could breach the gap from the cave surfaces to the sensors and that any cave surface beta background signal seen by the sensors would be severely attenuated.

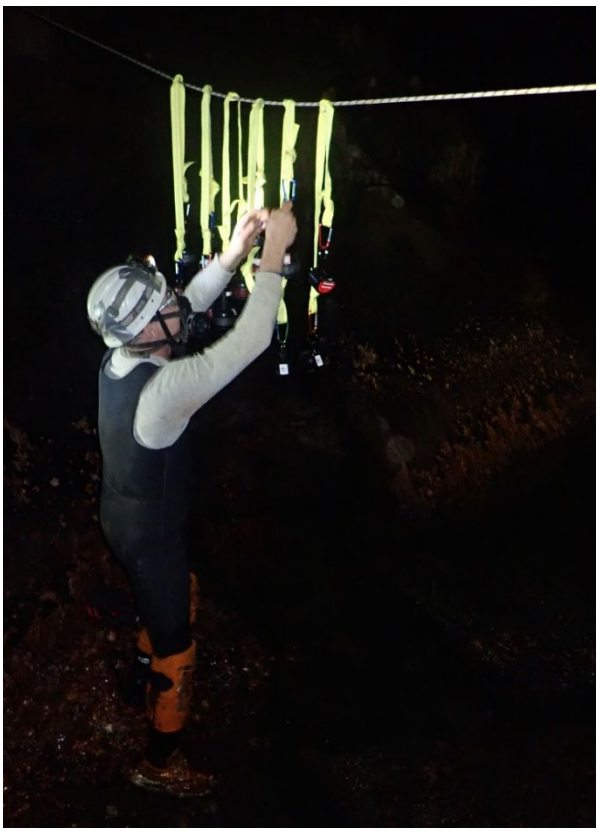

Figure (3): Setting up the hanging sensors, Coldwater Cave, station 4. Photo courtesy of Mark Jones.

Table 7 summarizes the data from the hanging sensor trial compared to control trials where the sensors were placed directly on the rock surfaces. Interpretation of the Table 7 information is not straightforward. Past trials at this location made it clear that ^{222}Rn varies in concentration as a function of time, but not rapidly (Welch, 2021). Within the time frame of each experimental trial, the ^{222}Rn had only minimal variation in concentration, as confirmed by Recon CRM temporal data. During the longer time frame of comparing one trial to the next (all collected on different dates), the concentration changed, often by a substantial amount. The air masses in the cave move, and that causes fresh gas sampling volumes that are either richer or poorer in ^{222}Rn to displace the previous air volume. Given the shorter half-life of ^{220}Rn, it should be less impacted by the movement of air masses, but it seems unreasonable to expect it to remain at a constant concentration over time. The cave surfaces remain essentially constant, short of things like violent flooding events. As such, the radiation background from these surfaces should remain at close to constant values. The hanging sensor trial in Coldwater Cave had a relative gap between the calculated RT chamber concentration and the S chamber concentration that was considerably higher than that from any of the control trials. If radiation from cave surfaces were a significant

factor, it would be expected to have been minimized in the hanging sensor trial, producing a smaller relative gap between RT and S. So, cave surface radiation seemed unlikely as a significant background component, echoing the results of the modified-RT experiments. Whether the background radiation from airborne particulates was a significant factor could not be addressed from this work, and future studies and different experimental approaches will be needed for this to be determined.

Table 7: Hanging sensor data vs. controls at the same site, Coldwater Cave, station 4.

Trial Type	RT Average (pCi/L)	S Average (pCi/L)	Absolute Difference (pCi/L)	Relative Difference (%)
Hanging Sensor Trial	413.6	344.0	69.6	20.2
Control Trial 1	481.1	429.7	51.4	12.0
Control Trial 2	610.1	566.5	43.6	7.70
Control Trial 3	499.4	473.4	26.0	5.49
Control Trial 4	439.2	425.2	14.0	3.29

Conclusions

Construction of the RT chamber for the E-PERM EIC system does change the degree of shielding of the sensor from external beta and gamma radiation. This is only a factor for radiation that has a linear path to enter the Tyvek-covered pores on the sides of the sensor, and only for intense beta and gamma sources a short distance from the pores. There is no evidence that background radiation from surfaces in the study caves was contributing to the difference in signal observed by RT chamber E-PERM units when compared to S chamber E-PERM units. If one is sampling in a potentially high radiation environment, it is recommended that the sensors be mounted on tripods or similar platforms to isolate them from potential beta and gamma producing surfaces. Radiation from airborne particulates closely approaching the RT chamber pores cannot be ruled out as contributing to the E-PERM signal. Most sampling environments are unlikely to provide sufficient particulate burden for this to make a difference, but further work is needed to evaluate the risks of background signal from particulate betas and gammas at sampling sites with high particulate burdens.

Acknowledgements

This study would not have been possible without the generous access privileges granted by the landowners of the study caves. Knox College provided financial support to enable this research. Experimental and theoretical assistance was provided by Ole Forsburg, Chuck Schulz, Judy Thorn, and the folks at Rad Elec. The photo in Figure 3 was provided courtesy of Mark Jones.

References

CERTI (Center for Environmental Research and Technology), 2006. Becoming Proficient with Rad Elec E-PERM® Measurement Devices.

Ionactive, 2021. Distance travelled by beta particles in air and other materials. Retrieved 2022-09-21: https://ionactive.co.uk/resource-hub/guidance/distance-travelled-by-beta-particles-in-air-and-other-materials.

Kotrappa, P., Dempsey, J.C., Hickey, J.R., and Stieff, L.R., 1988. An Electret Passive Environmental ^{222}Rn Monitor Based on Ionization Measurement. Health Physics, 54(1), 47-56.

Kotrappa, P., Dempsey, J.C., Ramsey, R.W., and Stieff, L.R., 1990. A Practical E-PERM™ (Electret Passive Environmental Radon Monitor) System for Indoor ^{222}Rn Measurement. Health Physics, 58(4), 461-467.

Kotrappa, P. and Steck, D., 2010. Electret Ion Chamber-Based Passive Radon-Thoron Discriminative Monitors. Radiation Protection Dosimetry, 141 (4), 386-389.

Kotrappa, P., Stieff, L., and Stieff, F., 2014. Attenuation of Thoron (^{220}Rn) in Tyvek Membranes. Proceedings of the 2014 International Radon Symposium, pp. 1-9. https://aarst.org/proceedings/2014/12_Kotrappa_ATTENUATION_OF_THORON_Rn220_IN_TYVEK_MEMBRANES.pdf.

Rumble, J.R., Editor-in-Chief, 2018. CRC Handbook of Chemistry and Physics, 99th edition. CRC Press, Boca Raton, Section 11.

Stacks, A.M. ed., 2015. Radon: Geology, Environmental Impact and Toxicity Concerns. Nova Science Pub., Hauppauge, NY, pp. 1-42.

Welch, L.E., Paul, B.E., and Jones, M.D., 2015. Measurement of Radon Levels in Caves: Logistical Hurdles and Solutions. Proceedings of the 2015 International Radon Symposium, pp. 1-17. http://aarst-nrpp.com/proceedings/2015/MEASUREMENT_OF_RADON LEVELS_IN_CAVES LOGISTICAL_HURDLES_AND_SOLUTIONS.pdf.

Welch, L.E., Paul, B.E., and Jones, M.D., 2016. Use of Electret Ionization Chambers to Measure Radon in Caves. Proceedings of the 2016 International Radon Symposium, pp. 1-18. http://aarst-nrpp.com/proceedings/2016/Welch_USE_OF_ELECTRET IONIZATION_CHAMBERS_TO_MEASURE_RADON_IN_CAVES.pdf.

Welch, L.E., Paul, B.E., Miller, E.C., Chen, Y.I., Jones, M.D., and Beck, C.L., 2017. Depth Profiling of Radon in Vertical Shafts Using Electret Ionization Chambers. Proceedings of the 2017 International Radon Symposium, pp. 1-18. http://http://aarst-nrpp.com/proceedings/2017/DEPTH-PROFILING-OF-RADON-IN-VERTICAL-SHAFTS-USING-ELECTRET-IONIZATION-CHAMBERS-WELCH.pdf.

Welch, L.E., Takashima, A., Miguel, M.B., Layug, B.C., Jones, M.D., and Beck, C.L, 2018. Correlating Environmental Variables with Radon Activity in an Iowa Cave. Proceedings of the 2018 International Radon Symposium, pp. 1-20. http://aarst-nrpp.com/proceedings/2018/Welch-CORRELATING-ENVIRONMENTAL-VARIABLES-WITH-RADON-ACTIVITY-IN-AN-IOWA-CAVE-2018.pdf.

Welch, L.E., Chen, Y.I, Jones, M.D., and Beck, C.L., 2019. Correlating Radon Activity with Carbon Dioxide Concentration in an Iowa Cave. Proceedings of the 2019 International Radon Symposium, pp. 11-25. https://aarst.org/proceedings/2019/CORRELATING-RADON-ACTIVITY-WITH-CARBON-DIOXIDE-CONCENTRATION-IN-IOWA-CAVE-WELCH-2019.pdf.

Welch, L.E., Paul, B.E., Takashima, A., Rau, G.D., Beck, C.L., Klausner, E.C., Miller, E.R., Jones, M.D., and Lace, M.J., 2021. Contextualizing Radon Activity in Northeastern Iowa Caves by Measuring Uranium and Thorium at the Radon Sampling Sites. Proceedings of the 2021 International Radon Symposium, pp. 1-14. https://aarst.org/proceedings/2021/Welch_Contextualizing-Radon-Activity-in-Northeastern-Iowa-Caves-2021.pdf.